

Ising spins coupled to a four-dimensional discrete Regge skeleton

E. Bittner

Atominstitut der Österreichischen Universitäten, TU Wien, A-1040 Vienna, Austria

Institut für Theoretische Physik, Universität Leipzig, D-04109 Leipzig, Germany

W. Janke

Institut für Theoretische Physik, Universität Leipzig, D-04109 Leipzig, Germany

H. Markum

Atominstitut der Österreichischen Universitäten, TU Wien, A-1040 Vienna, Austria

(October 20, 2018)

Abstract

Regge calculus is a powerful method to approximate a continuous manifold by a simplicial lattice, keeping the connectivities of the underlying lattice fixed and taking the edge lengths as degrees of freedom. The discrete Regge model employed in this work limits the choice of the link lengths to a finite number. To get more precise insight into the behavior of the four-dimensional discrete Regge model, we coupled spins to the fluctuating manifolds. We examined the phase transition of the spin system and the associated critical exponents. The results are obtained from finite-size scaling analyses of Monte Carlo simulations. We find consistency with the mean-field theory of the Ising model on a static four-dimensional lattice.

PACS: 04.60.Nc, 05.50.+q

Typeset using REVTeX

I. INTRODUCTION

Spin systems coupled to fluctuating manifolds are analyzed as a simple example for matter fields coupled to Euclidean quantum gravity. The gravitational action is unbounded from below due to conformal fluctuations. But that does not necessarily render its quantum theory useless or the path integral undefined. Indeed, the existence of a well defined phase was the first and probably most important result of the numerical simulations in four dimensions [1,2]. Its existence and stability were explored in some detail using the standard Regge calculus with continuous link lengths. It turned out that the well defined phase is stable against variations of the measure and the lattice size [3].

In the discrete Regge model the problem of an unbounded action is not present as in standard Regge calculus. Because of the restriction of possible quadratic link lengths to two values [4,5] in the discrete Regge model the action can only reach an extreme but finite value. The expectation values do not diverge if the well defined phase is left. What happens is that the lattice “freezes” at large positive and negative values of the gravitational coupling, as expected for a spin system [6]. To get more precise ideas about the behavior of the four-dimensional discrete Regge model, we coupled Ising spins to the fluctuating manifolds. We examined the phase transition of the spin system and the associated critical exponents.

The rest of the paper is organized as follows. In Sec. II we introduce the discrete Regge model and give some details of the analyzed observables. The results of the Monte Carlo simulations are presented in Sec. III, and concluding remarks can be found in Sec. IV.

II. MODELS AND OBSERVABLES

The situation for the discrete Regge model is both structurally and computationally much simpler than the standard Regge calculus with continuous link lengths. The restriction of the edge lengths to just two values was carefully examined in 2D where an interpolation from Z_2 to Z_∞ was performed [7]. It turned out that the phase transition with respect to the

cosmological constant is universal. This was tested for pure gravity in 2D and is expected to be the case also in 4D. Compared with standard Regge calculus, numerical simulations of the discrete Regge model can be done more efficiently by implementing look-up tables and using the heat-bath algorithm. In the actual computations we took the squared link lengths as $q_{ij} \equiv q_l = b_l(1 + \epsilon\sigma_l)$ with $\sigma_l \pm 1$. The Euclidean triangle inequalities are satisfied automatically as long as $\epsilon < \epsilon_{\max}$. Because a four-dimensional Regge skeleton with equilateral simplices cannot be embedded in flat space, b_l takes different values depending on the type of the edge l . In particular $b_l = 1, 2, 3, 4$ for edges, face diagonals, body diagonals, and the hyperbody diagonal of a hypercube.

We investigated the partition function

$$Z = \sum_{\{s\}} \int D[q] \exp[-I(q) - KE(q, s)], \quad (2.1)$$

where $I(q)$ is the gravitational action,

$$I(q) = -\beta_g \sum_t A_t \delta_t + \lambda \sum_i V_i. \quad (2.2)$$

The first sum runs over all products of triangle areas A_t times corresponding deficit angles δ_t weighted by the gravitational coupling β_g . The second sum extends over the volumes V_i of the 4-simplices of the lattice and allows one together with the cosmological constant λ to set an overall scale in the action. The energy of Ising spins $s_i \in Z_2$,

$$E(q, s) = \frac{1}{2} \sum_{\langle ij \rangle} A_{ij} \frac{(s_i - s_j)^2}{q_{ij}}, \quad (2.3)$$

is defined as in two dimensions [8–10], with the barycentric area A_{ij} associated with a link l_{ij} ,

$$A_{ij} = \sum_{t \supset l_{ij}} \frac{1}{3} A_t. \quad (2.4)$$

We chose the simple uniform measure as in the pure gravity simulations [6]:

$$D[q] = \prod_l dq_l \mathcal{F}(q_l). \quad (2.5)$$

The function \mathcal{F} ensures that only Euclidean link configurations are taken into account, i.e., $\mathcal{F} = 1$ if the Euclidean triangle inequalities are fulfilled and $\mathcal{F} = 0$ otherwise. This is always guaranteed for the discrete Regge model by construction.

For every Monte Carlo simulation run we recorded the time series of the energy density $e = E/N_0$ and the magnetization density $m = \sum_i s_i/N_0$, with the lattice size $N_0 = L^4$. To obtain results for the various observables \mathcal{O} at values of the spin coupling K in an interval around the simulation point K_0 , we applied the reweighting method [11]. Since we recorded the time series, this amounts to computing

$$\langle \mathcal{O} \rangle|_K = \frac{\langle \mathcal{O} e^{-\Delta KE} \rangle|_{K_0}}{\langle e^{-\Delta KE} \rangle|_{K_0}}, \quad (2.6)$$

with $\Delta K = K - K_0$.

With the help of the time series we can compute the specific heat,

$$C(K) = K^2 N_0 (\langle e^2 \rangle - \langle e \rangle^2), \quad (2.7)$$

the (finite lattice) susceptibility,

$$\chi(K) = N_0 (\langle m^2 \rangle - \langle |m| \rangle^2), \quad (2.8)$$

and various derivatives of the magnetization, $d\langle |m| \rangle/dK$, $d\ln\langle |m| \rangle/dK$, and $d\ln\langle m^2 \rangle/dK$. All these quantities exhibit in the infinite-volume limit singularities at K_c which are shifted and rounded in finite systems. We further analyzed the Binder parameter,

$$U_L(K) = 1 - \frac{1}{3} \frac{\langle m^4 \rangle}{\langle m^2 \rangle^2}. \quad (2.9)$$

It is well known that the $U_L(K)$ curves for different lattice sizes L cross around (K_c, U^*) . This allows an almost unbiased estimate of the critical spin coupling K_c .

III. SIMULATION RESULTS

In four dimensions, after initial discussions [12–14] it is generally accepted that the critical properties of the Ising model on a static lattice are given by mean-field theory with logarithmic corrections. The finite-size scaling (FSS) formulas can be written as [15,16]

$$\xi \propto L(\log L)^{\frac{1}{4}}, \quad (3.1)$$

$$\chi \propto L^2(\log L)^{\frac{1}{2}} = (L(\log L)^{\frac{1}{4}})^{\gamma/\nu}, \quad (3.2)$$

$$C \propto (\log L)^{\frac{1}{3}}, \quad (3.3)$$

$$K_c(\infty) - K_c(L) \propto L^{-2}(\log L)^{-\frac{1}{6}} = (L(\log L)^{\frac{1}{12}})^{-1/\nu}, \quad (3.4)$$

where the critical exponents of mean-field theory are $\alpha = 0$, $\beta = 1/2$, $\gamma = 1$, and $\nu = 1/2$. To get more precise ideas about these logarithmic corrections, we first simulated the four-dimensional Ising model on a regular lattice. After this comparative study we turned to the four-dimensional discrete Regge model [6] with spin fields.

A. Ising spins on a regular lattice

We studied the four-dimensional Ising model on a hypercubic lattice with linear size $L = 3 - 16, 18, 20, 24, 28, 32, 36, 40$, using the single-cluster update algorithm (Wolff) [17]. The simulations were performed with the knowledge of the value of the critical temperature obtained in previous Monte Carlo simulations and high-temperature series analyses [18]:

$$K_c = \frac{J}{k_B T_c} = 0.149\,694 \pm 0.000\,002. \quad (3.5)$$

We performed $n(L) \propto N_0/\langle C(L) \rangle$ cluster updates between measurements for lattices $L \leq 24$, with the averaged cluster size $\langle C(L) \rangle$. After an initial equilibration time of about $1\,000 \times n(L)$ cluster updates we took about 50 000 measurements for each of the small lattices. For the larger lattices we measured after each cluster update, therefore, we took about 500 000 measurements after an initial equilibration of 100 000 cluster updates. Analyzing the time series we found integrated autocorrelation times for the energy and the magnetization in the range of unity for the small lattices $L \leq 24$ and in the range of $(4 - 8) \times L$ for the larger lattice sizes. The statistical errors were obtained by the standard jack-knife method using 50 blocks.

Applying the reweighting technique we first determined the maxima of C , χ , $d\langle |m| \rangle/dK$, $d\ln\langle |m| \rangle/dK$, and $d\ln\langle m^2 \rangle/dK$. The locations of the maxima provide us with five se-

quences of pseudo-transition points $K_{\max}(L)$ for which the scaling variable $x = (K_c - K_{\max}(L))(L(\log L)^{\frac{1}{12}})^{1/\nu}$ should be constant. Using this fact we then have several possibilities to extract the critical exponent ν from (linear) least-square fits of the FSS ansatz with multiplicative logarithmic corrections considering Eq. (3.4),

$$dU_L/dK \cong (L(\log L)^{\frac{1}{12}})^{1/\nu} f_0(x) \quad \text{or} \quad (3.6)$$

$$d\ln\langle|m|^p\rangle/dK \cong (L(\log L)^{\frac{1}{12}})^{1/\nu} f_p(x), \quad (3.7)$$

to the data at the various $K_{\max}(L)$ sequences. For comparison we also performed fits of a naive power-law FSS ansatz

$$dU_L/dK \cong L^{1/\nu} f_0(x) \quad \text{or} \quad (3.8)$$

$$d\ln\langle|m|^p\rangle/dK \cong L^{1/\nu} f_p(x). \quad (3.9)$$

The exponents $1/\nu$ resulting from fits using the data for the N largest lattice sizes are collected in Tables I and II. Q denotes the standard goodness-of-fit parameter. For all exponent estimates the FSS ansatz with the logarithmic corrections leads to the weighted average $1/\nu = 1.993(3)$, which is in perfect agreement with the mean-field value $1/\nu = 2$, see Fig. 1 (a). With the naive power-law ansatz one also gets an estimate for $1/\nu$ in the vicinity of the mean-field value, but this is clearly separated from the mean-field result, verifying the significance of the multiplicative logarithmic correction, cf. Table II.

Assuming therefore $\nu = 0.5$ we can obtain estimates for K_c from linear least-square fits to the scaling behavior of the various K_{\max} sequences, as shown in Fig. 1 (b). Using the fits with $L \geq 12$, the combined estimate from the five sequences leads to $K_c = 0.149\,697(2)$, which is in agreement with the results using Monte Carlo computer simulations [18] and series expansions [19,20].

Knowing the critical coupling we may reconfirm our estimates of $1/\nu$ by evaluating the above quantities at K_c . As can be seen in Tables I and II, the statistical errors of the FSS fits at K_c are similar to those using the K_{\max} sequences. However, the uncertainty in the estimate of K_c has also to be taken into account. This error is computed by repeating the

fits at $K_c \pm \Delta K_c$ and indicated in Tables I and II by the numbers in square brackets. In the computation of the weighted average we assume the two types of errors to be independent. As a result of this combined analysis we obtain strong evidence that the exponent ν agrees with the mean-field value of $\nu = 0.5$.

To extract the critical exponent ratio γ/ν we use the scaling

$$\chi_{\max} \cong (L(\log L)^{\frac{1}{4}})^{\gamma/\nu} \quad (3.10)$$

as well as the scaling of χ at K_c , yielding in the range $L = 10-40$ estimates of $\gamma/\nu = 2.037(9)$ with $Q = 0.95$ and $\gamma/\nu = 2.008(5)[5]$ ($Q = 0.46$), respectively. These estimates for γ/ν are consistent with the mean-field value of $\gamma/\nu = 2$. In Fig. 2 (a) this is demonstrated graphically by comparing the scaling of χ_{\max} with a constrained one-parameter fit of the form $\chi_{\max} = c(L(\log L)^{\frac{1}{4}})^2$ with $c = 0.526(2)$ ($Q = 0.38$, $L \geq 6$).

Concerning the specific heat we expect in the case of the mean-field exponent $\alpha = 0$ a logarithmic divergence of the form

$$C(x, L) = A(x) + B(x)(\log L)^{\frac{1}{3}}. \quad (3.11)$$

Indeed, the data at the different fixed values of x can all be fitted nicely with this ansatz. In particular, for the fit of C_{\max} with 17 points ($L \geq 6$) we obtain $A = -0.324(32)$, $B = 1.038(23)$, with a total $\chi^2 = 11.7(Q = 0.70)$. We also tried an unbiased three-parameter fit using the ansatz

$$C(x, L) = A'(x) + B'(x)(\log L)^{\kappa(x)}, \quad (3.12)$$

which in the case of the fit of C_{\max} and 16 data points gives $A' \approx -0.36$, $B' \approx 1.75$, and $\kappa = 0.33(40)$, with a slightly improved total $\chi^2 = 10.8(Q = 0.62)$. In Fig. 2 (b) we compare these two linear least-square fits. It should be noted, however, that the three-parameter fit is highly unstable and exhibits strong correlations between the three parameters. To illustrate this instability we plot in Fig. 3 (a) the exponent κ as a function of the smallest lattice size L_{\min} , being the lower bound of the fit range $[L_{\min}, 40]$. For comparison we show in Fig. 3 (b) the behavior of γ/ν results of the fit corresponding to Eq. (3.10).

fit type	N	$1/\nu$	Q
dU/dK at K_{\max}^C	22	1.990(5)	0.68
$d\ln\langle m \rangle/dK$ at $K_{\inf}^{\ln\langle m \rangle}$	18	1.989(4)	0.94
$d\ln\langle m^2\rangle/dK$ at $K_{\inf}^{\ln\langle m^2\rangle}$	18	1.998(5)	0.93
weighted average		1.993(3)	
dU/dK at K_c	18	1.991(5)[1]	0.73
$d\ln\langle m \rangle/dK$ at K_c	18	1.992(5)[2]	0.94
$d\ln\langle m^2\rangle/dK$ at K_c	18	2.000(5)[2]	0.94
weighted average		1.995(3)	
overall average		1.994(2)	

Table I. Fit results for $1/\nu$ with a power-law ansatz with logarithmic corrections, using the data for the N largest lattices. The average is computed by weighting each entry with its inverse squared error. For the fits at our best estimate of $K_c = 0.149\,697(2)$ the uncertainty due to the error in K_c is indicated by the numbers in square brackets.

fit type	N	$1/\nu$	Q
dU/dK at K_{\max}^C	18	2.041(9)	0.81
$d\ln\langle m \rangle/dK$ at $K_{\inf}^{\ln\langle m \rangle}$	18	2.056(5)	0.75
$d\ln\langle m^2\rangle/dK$ at $K_{\inf}^{\ln\langle m^2\rangle}$	18	2.066(5)	0.63
weighted average		2.059(3)	
dU/dK at K_c	18	2.043(9)[2]	0.81
$d\ln\langle m \rangle/dK$ at K_c	18	2.059(5)[2]	0.81
$d\ln\langle m^2\rangle/dK$ at K_c	18	2.067(5)[2]	0.70
weighted average		2.061(4)	
overall average		2.060(2)	

Table II. Fit results for $1/\nu$ with a pure power-law ansatz using $K_c = 0.149\,697(2)$. The averages and statistical errors are computed as in Table I.

FIGURES

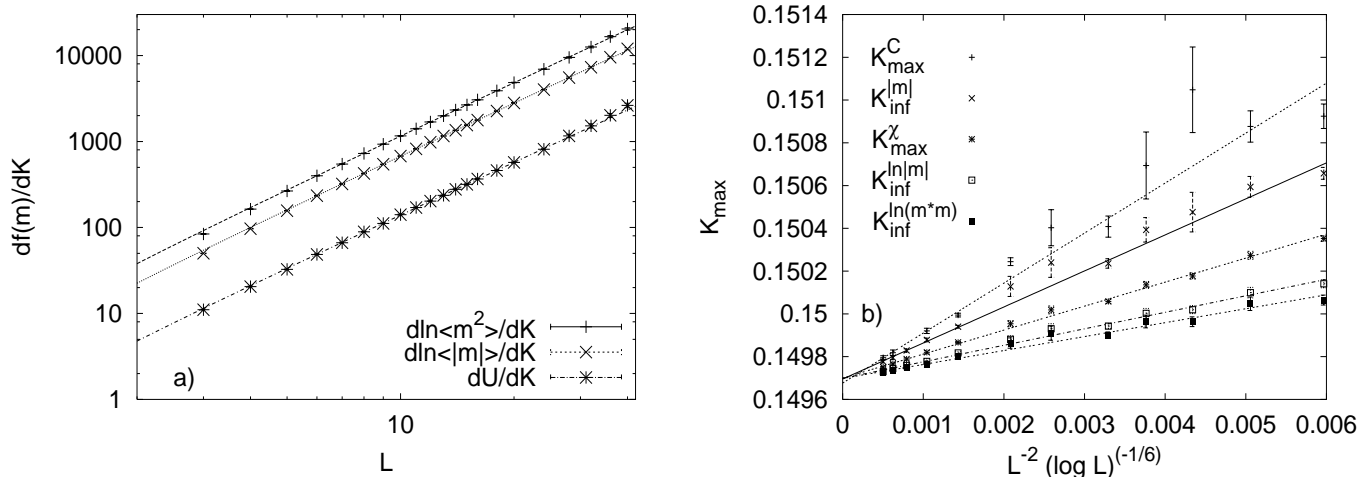


FIG. 1. (a) Least-square fits of the FSS ansatz with logarithmic corrections at the maxima locations. Together with the fits at K_c this leads to an overall critical exponent $1/\nu = 1.994(2)$. (b) FSS extrapolations of pseudo-transition points K_{\max} vs. $(L(\log L)^{\frac{1}{12}})^{-1/\nu}$, assuming $\nu = 0.5$. The error-weighted average of extrapolations to infinite size yields $K_c = 0.149697(2)$.

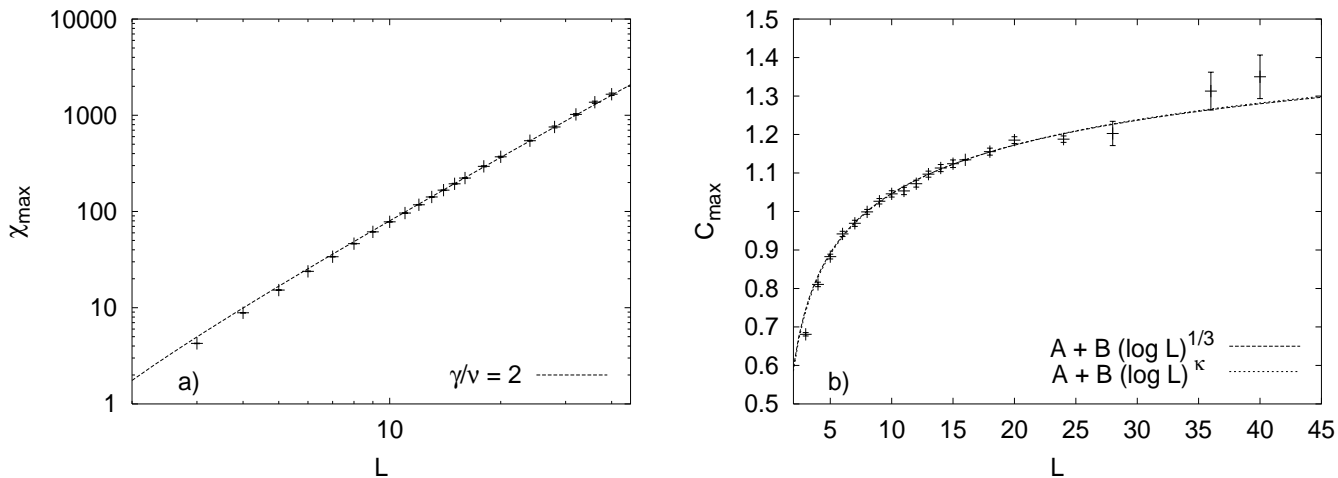


FIG. 2. (a) FSS of the susceptibility maxima χ_{\max} . The exponent entering the curve is set to the mean-field value $\gamma/\nu = 2$ for regular static lattices. (b) FSS of the specific-heat maxima C_{\max} . The logarithmic fit $C_{\max} = A + B(\log L)^{\kappa}$ and a constrained logarithmic fit assuming the mean-field prediction $\kappa = 1/3$ are almost indistinguishable on the scale of the figure.

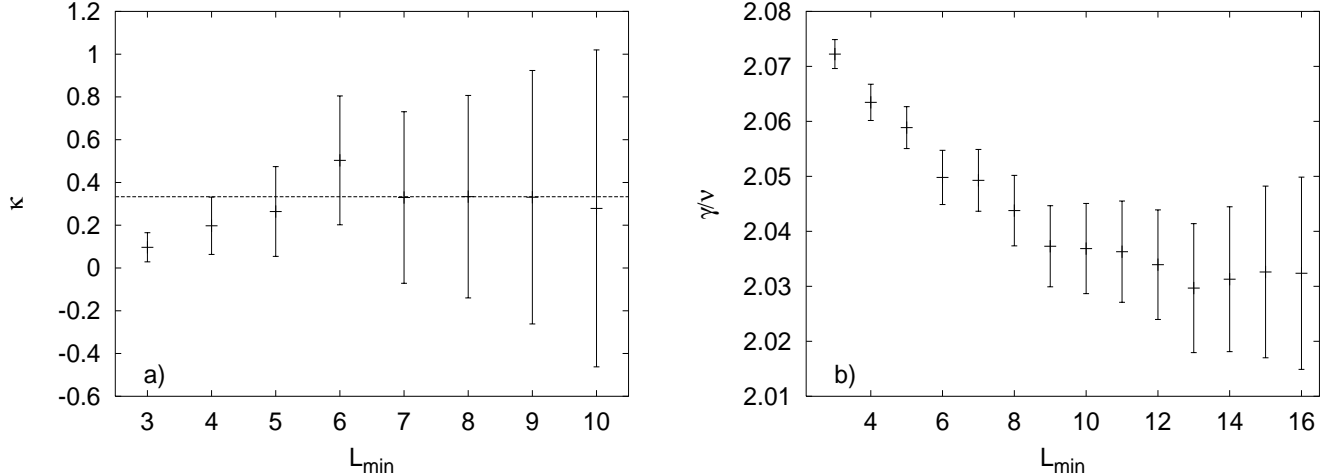


FIG. 3. (a) Instability of the logarithmic fit $C_{\max} = A + B(\log L)^\kappa$. The exponent κ as a function of the lower bound of the fit range is plotted. (b) γ/ν as a function of the lower bound of the fit range is plotted for the fit $\chi_{\max} \propto (L(\log L)^{\frac{1}{4}})^{\gamma/\nu}$.

B. Ising spins on a discrete Regge model

We simulated the gravitational degrees of freedom (the squared link lengths) of the partition function (2.1) using the heat-bath algorithm. For the Ising spins we employed again the single-cluster algorithm. Between measurements we performed $n = 10$ Monte Carlo steps consisting of one lattice sweep to update the squared link lengths q_{ij} followed by two single-cluster flips to update the spins s_i .

The simulations were done for $\epsilon = 0.0875$, cosmological constant $\lambda = 0$ and two different gravitational couplings, $\beta_g = -4.665$ and $\beta_g = 22.3$. These two β_g -values correspond to the two phase transitions of the pure discrete Regge model [6], as shown in Fig. 4. The transition at positive gravitational coupling of the standard Regge calculus was described in great detail in Ref. [21] and shown to be of first order whereas the transition at negative coupling turned out to be of second order for the discrete Regge model [6]. Together with an eventual second-order transition of the Ising part, the latter one is a candidate for a possible continuum limit. The lattice topology is given by triangulated tori of size $N_0 = L^4$ with $L = 3$ up to 10. From short test runs we estimated the location of the phase transition of

the spin model and set the spin coupling $K_0 = 0.024 \approx K_c$ in the long runs for both values of β_g , see Fig. 5.

After an initial equilibration time we took about 100 000 measurements for each lattice size. Analyzing the time series we found integrated autocorrelation times for the energy and the magnetization in the range of unity for all considered lattice sizes. As in the simulations of the regular lattices the statistical errors were obtained by the standard jack-knife method using 50 blocks.

Completely analogously to the Ising system on a regular lattice we applied reweighting to locate the maxima and used the FSS formulas (3.6)–(3.9). The exponents $1/\nu$ resulting from fits using the data for the N largest lattice sizes are collected in Tables III and IV for $\beta_g = -4.665$, and in Tables V and VI for $\beta_g = 22.3$, respectively. For the simulations at $\beta_g = -4.665$ all exponent estimates with the logarithmic corrections and consequently also their weighted average $1/\nu = 2.025(6)$ are in agreement with the mean-field value $1/\nu = 2$, see Fig. 6 (a). For $\beta_g = 22.3$ the scatter in the estimates is similar and the weighted average $1/\nu = 2.028(6)$ is again compatible with $1/\nu = 2$. With the naive power-law ansatz one also gets an estimate for $1/\nu$ in the vicinity of the mean-field value, but this is clearly separated from the mean-field result, cf. Tables IV and VI.

Assuming therefore $\nu = 0.5$ we can obtain estimates for K_c from linear least-square fits to the scaling behavior of the various K_{\max} sequences, as shown in Fig. 6 (b) for $\beta_g = -4.665$. Using the fits with $L \geq 4$, the combined estimate from the five sequences leads to $K_c = 0.02464(4)$ for $\beta_g = -4.665$, and for $\beta_g = 22.3$ we find $K_c = 0.02339(4)$, again with $L \geq 4$.

With the knowledge of the critical couplings we may reconfirm our estimates of $1/\nu$ by evaluating the above quantities at K_c . As can be inspected in Tables III and V, we obtain from this combined analysis strong evidence that the exponent ν agrees with the mean-field value of $\nu = 0.5$.

To extract the critical exponent ratio γ/ν we use the FSS formula (3.10) for χ_{\max} as well as the scaling of χ at K_c , yielding for $\beta_g = -4.665$ in the range $L = 4 - 10$ estimates

of $\gamma/\nu = 2.039(9)$ with $Q = 0.42$ and $\gamma/\nu = 2.036(7)[4]$ ($Q = 0.85$), respectively. The corresponding values for $\beta_g = 22.3$, using the same fit range, are $\gamma/\nu = 2.052(8)$ ($Q = 0.57$) and $\gamma/\nu = 2.052(6)[4]$ ($Q = 0.01$). These estimates for γ/ν are compatible with the mean-field value of $\gamma/\nu = 2$. In Fig. 7 (a) this is demonstrated by comparing the scaling of χ_{\max} with a constrained one-parameter fit of the form $\chi_{\max} = c(L(\log L)^{\frac{1}{4}})^2$ with $c = 4.006(10)$ ($Q = 0.17, L \geq 6$) for $\beta_g = -4.665$ and $c = 4.244(10)$ ($Q = 0.001, L \geq 6$) for $\beta_g = 22.3$, respectively.

The data for the specific heat C at the critical spin coupling K_c are presented in Fig. 7 (b). The fact that C increases very slowly with the size of the lattice means that one will need data from bigger lattices and more statistical accuracy to get an estimate or bound for the critical exponent α from a direct measurement of C . Especially, if we assume a logarithmic divergence of C as in the four-dimensional Ising model on regular lattices, we need lattices of comparable size, cf. Fig. 2 (b).

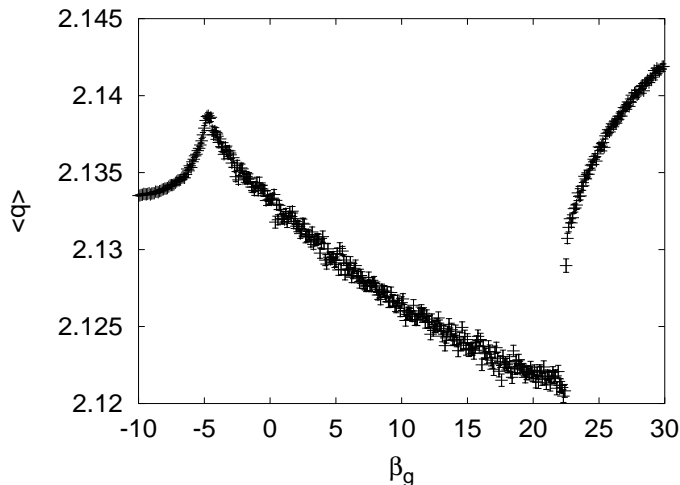


FIG. 4. Expectation values of the average squared link lengths as a function of the gravitational coupling for the pure discrete Regge model on a 4^4 lattice.

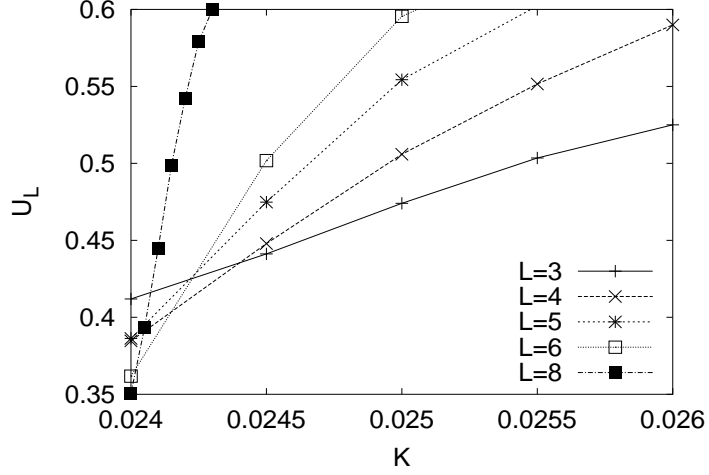


FIG. 5. Binder cumulant curves from the short runs at $\beta_g = -4.665$ leading to a critical spin coupling $K_c \approx K_0 = 0.024$.

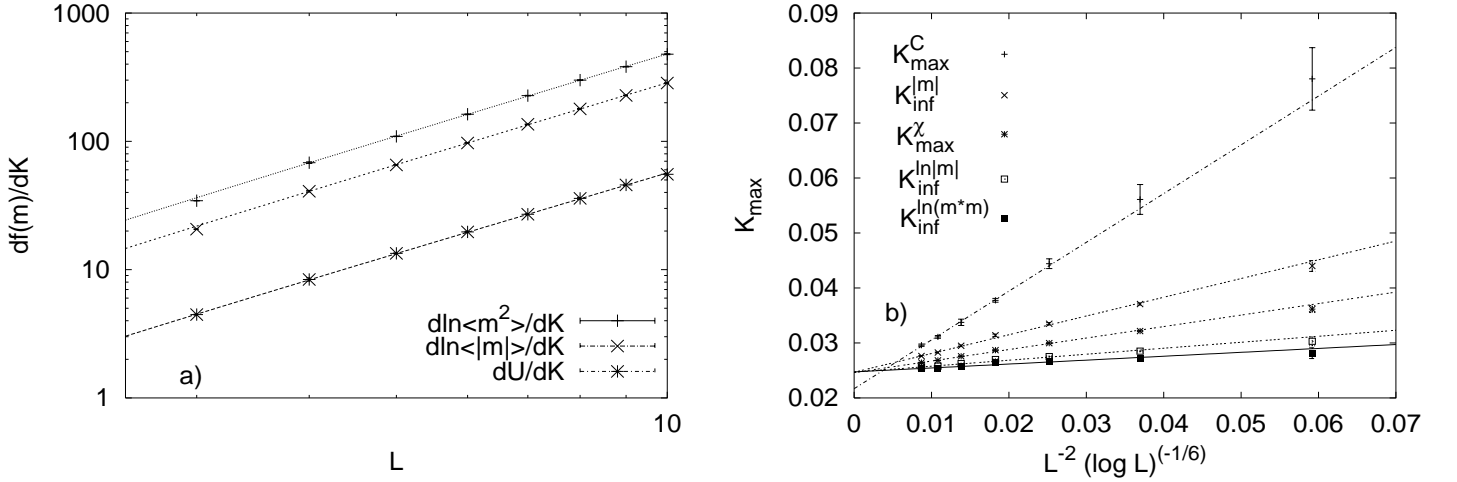


FIG. 6. (a) Least-square fits of the FSS ansatz with logarithmic corrections for $\beta_g = -4.665$ lead to an overall critical exponent $1/\nu = 2.025(4)$. (b) FSS extrapolations of pseudo-transition points K_{\max} vs. $(L(\log L)^{\frac{1}{12}})^{-1/\nu}$ for $\beta_g = -4.665$, assuming $\nu = 0.5$. The error-weighted average of extrapolations to infinite size yields $K_c = 0.02464(4)$.

fit type	N	$1/\nu$	Q
dU/dK at K_{\max}^C	8	2.003(10)	0.47
$d\ln\langle m \rangle/dK$ at $K_{\inf}^{\ln\langle m \rangle}$	7	2.032(10)	0.59
$d\ln\langle m^2\rangle/dK$ at $K_{\inf}^{\ln\langle m^2\rangle}$	7	2.038(10)	0.55
weighted average		2.025(6)	
dU/dK at K_c	7	1.981(17)[13]	0.70
$d\ln\langle m \rangle/dK$ at K_c	7	2.027(9)[2]	0.95
$d\ln\langle m^2\rangle/dK$ at K_c	7	2.034(9)[2]	0.85
weighted average		2.025(6)	
overall average		2.025(4)	

Table III. Fit results for $1/\nu$ with a power-law ansatz with logarithmic corrections for $\beta_g = -4.665$, using the data for the N largest lattices. The average is computed by weighting each entry with its inverse squared error. For the fits at our best estimate of $K_c = 0.02464(4)$ the uncertainty due to the error in K_c is indicated by the numbers in square brackets.

fit type	N	$1/\nu$	Q
dU/dK at K_{\max}^C	7	2.068(18)	0.60
$d\ln\langle m \rangle/dK$ at $K_{\inf}^{\ln\langle m \rangle}$	7	2.122(10)	0.37
$d\ln\langle m^2\rangle/dK$ at $K_{\inf}^{\ln\langle m^2\rangle}$	7	2.128(10)	0.35
weighted average		2.118(7)	
dU/dK at K_c	7	2.068(18)[12]	0.59
$d\ln\langle m \rangle/dK$ at K_c	7	2.116(9)[2]	0.83
$d\ln\langle m^2\rangle/dK$ at K_c	7	2.124(9)[2]	0.64
weighted average		2.116(7)	
overall average		2.117(5)	

Table IV. Fit results for $1/\nu$ with a pure power-law ansatz for $\beta_g = -4.665$. The averages and statistical errors are computed as in Table III.

fit type	N	$1/\nu$	Q
dU/dK at K_{\max}^C	8	1.981(10)	0.64
$d\ln\langle m \rangle/dK$ at $K_{\inf}^{\ln\langle m \rangle}$	7	2.043(9)	0.61
$d\ln\langle m^2\rangle/dK$ at $K_{\inf}^{\ln\langle m^2\rangle}$	7	2.049(9)	0.67
weighted average		2.028(6)	
dU/dK at K_c	8	1.993(10)[1]	0.76
$d\ln\langle m \rangle/dK$ at K_c	7	2.039(9)[2]	0.32
$d\ln\langle m^2\rangle/dK$ at K_c	7	2.045(9)[2]	0.49
weighted average		2.027(6)	
overall average		2.028(4)	

Table V. Fit results for $1/\nu$ with a power-law ansatz with logarithmic corrections for $\beta_g = 22.3$. The average is computed by weighting each entry with its inverse squared error. For the fits at our best estimate of $K_c = 0.02339(4)$ the uncertainty due to the error in K_c is indicated by the numbers in square brackets.

fit type	N	$1/\nu$	Q
dU/dK at K_{\max}^C	7	2.086(11)	0.72
$d\ln\langle m \rangle/dK$ at $K_{\inf}^{\ln\langle m \rangle}$	7	2.134(10)	0.54
$d\ln\langle m^2\rangle/dK$ at $K_{\inf}^{\ln\langle m^2\rangle}$	7	2.139(9)	0.59
weighted average		2.122(6)	
dU/dK at K_c	8	2.098(10)[1]	0.57
$d\ln\langle m \rangle/dK$ at K_c	7	2.130(9)[2]	0.35
$d\ln\langle m^2\rangle/dK$ at K_c	7	2.135(9)[2]	0.48
weighted average		2.122(6)	
overall average		2.122(4)	

Table VI. Fit results for $1/\nu$ with a pure power-law ansatz for $\beta_g = 22.3$. The averages and statistical errors are computed as in Table V.

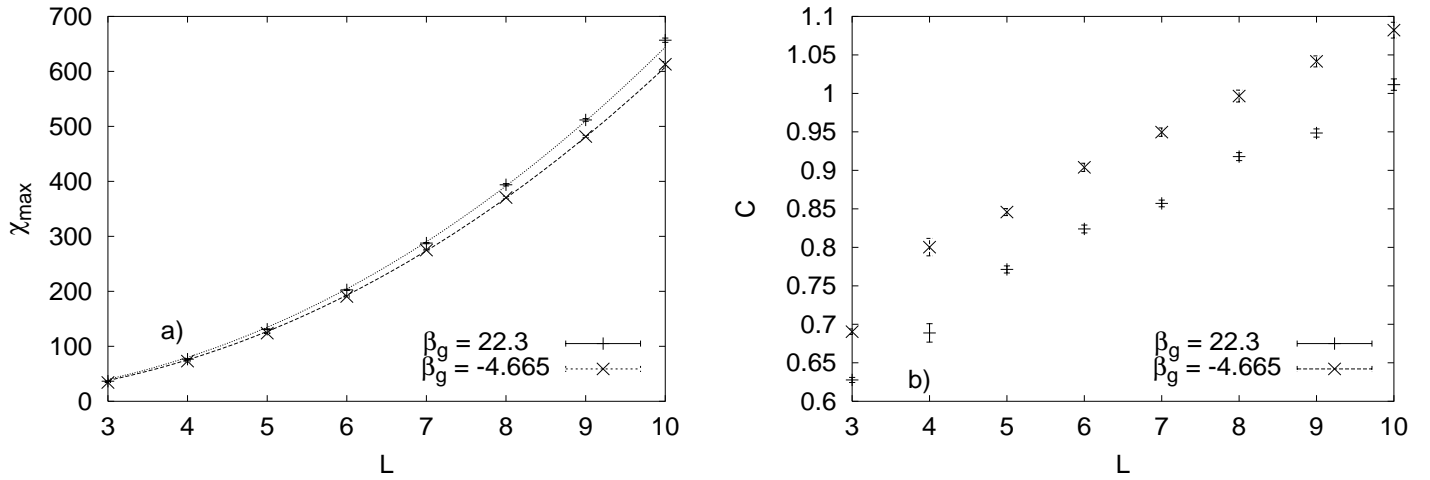


FIG. 7. (a) FSS of the susceptibility maxima χ_{\max} . The exponent entering the curve is set to the mean-field value $\gamma/\nu = 2$ for regular static lattices. (b) Specific heat at the critical spin coupling as a function of the lattice size L .

IV. CONCLUSIONS

We have performed a study of the Ising model coupled to fluctuating manifolds via Regge calculus. Analyzing the discrete Regge model with two permissible edge lengths it turns out that the Ising transition shows the predicted logarithmic corrections to the mean-field theory. The critical exponents of the phase transition of the Ising spins on a static lattice as well as on a discrete Regge skeleton [22] are consistent with the exponents of the mean-field theory, $\alpha = 0$, $\beta = \frac{1}{2}$, $\gamma = 1$, and $\nu = \frac{1}{2}$. In summary, our consistent analysis with uniform computer codes yields that the phase transition of a spin system coupled to a discrete Regge skeleton exhibits the same critical exponents and the same logarithmic corrections [16] as on a static lattice.

ACKNOWLEDGMENTS

E.B. was supported by Fonds zur Förderung der wissenschaftlichen Forschung under project P14435-TPH and thanks the Graduiertenkolleg “Quantenfeldtheorie: Mathematische Struktur und Anwendungen in der Elementarteilchen- und Festkörperphysik” for hospitality during his extended stay in Leipzig. W.J. acknowledges partial support by the EC IHP Network grant HPRN-CT-1999-00161: “EUROGRID”.

REFERENCES

- [1] H.W. Hamber, in Proceedings of the 1984 Les Houches Summer School, edited by K. Osterwalder and R. Stora, Session XLIII (North-Holland, Amsterdam, 1986); H.W. Hamber and R.M. Williams, Phys. Lett. B **157**, 368 (1985).
- [2] B.A. Berg, in *Particle Physics and Astrophysics*, Proceedings of the XXVII Int. Universitätswochen für Kernphysik, edited by H. Mitter and F. Widder (Springer, Berlin, 1989); Phys. Rev. Lett. **55**, 904 (1985); Phys. Lett. B **176**, 39 (1986).
- [3] W. Beirl, E. Gerstenmayer, H. Markum, and J. Riedler, Phys. Rev. D **49**, 5231 (1994).
- [4] W. Beirl, H. Markum, and J. Riedler, Int. J. Mod. Phys. C **5**, 359 (1994) and hep-lat/9312054.
- [5] T. Fleming, M. Gross, and R. Renken, Phys. Rev. D **50**, 7363 (1994).
- [6] W. Beirl, A. Hauke, P. Homolka, B. Krishnan, H. Kröger, H. Markum, and J. Riedler, Nucl. Phys. B (Proc. Suppl.) **47**, 625 (1996); W. Beirl, A. Hauke, P. Homolka, H. Markum, and J. Riedler, Nucl. Phys. B (Proc. Suppl.) **53**, 735 (1997); J. Riedler, W. Beirl, E. Bittner, A. Hauke, P. Homolka, and H. Markum, Class. Quantum Grav. **16**, 1163 (1999).
- [7] E. Bittner, H. Markum, and J. Riedler, Nucl. Phys. B (Proc. Suppl.) **73**, 789 (1999).
- [8] M. Gross and H.W. Hamber, Nucl. Phys. B **364**, 703 (1991).
- [9] C. Holm and W. Janke, Phys. Lett. B **335**, 143 (1994).
- [10] E. Bittner, W. Janke, H. Markum, and J. Riedler, Physica A **277**, 204 (2000).
- [11] A.M. Ferrenberg and R.H. Swendsen, Phys. Rev. Lett. **61**, 2635 (1988).
- [12] D.S. Gaunt, M.F. Sykes, and S. McKenzie, J. Phys. A **12**, 871 (1979).
- [13] S. McKenzie and D.S. Gaunt, J. Phys. A **13**, 1015 (1980).

- [14] E. Sánchez-Velasco, *J. Phys. A* **20**, 5033 (1987).
- [15] R. Kenna and C.B. Lang, *Phys. Lett. B* **264**, 396 (1991); *Nucl. Phys. B* **393**, 461 (1993).
- [16] H.G. Ballesteros, L.A. Fernández, V. Martín-Mayor, A. Muñoz Sudupe, G. Parisi, and J.J. Ruiz-Lorenzo, *Nucl. Phys. B* **512**, 681 (1998).
- [17] U. Wolff, *Phys. Rev. Lett.* **62**, 361 (1989); *Nucl. Phys. B* **322**, 759 (1989).
- [18] D. Stauffer and J. Adler, *Int. J. Mod. Phys. C* **8**, 263 (1997).
- [19] D.S. Gaunt, M.F. Sykes, and S. McKenzie, *J. Phys. A* **12**, L339 (1976).
- [20] J. Adler and D. Stauffer, *Int. J. Mod. Phys. C* **6**, 807 (1995).
- [21] H.W. Hamber, *Phys. Rev. D* **61**, 124008 (2000).
- [22] E. Bittner, W. Janke, and H. Markum, *Nucl. Phys. B (Proc. Suppl.)* **106-107**, 989 (2002).